PCCP

Accepted Manuscript

This is an *Accepted Manuscript*, which has been through the Royal Society of Chemistry peer review process and has been accepted for publication.

Accepted Manuscripts are published online shortly after acceptance, before technical editing, formatting and proof reading. Using this free service, authors can make their results available to the community, in citable form, before we publish the edited article. We will replace this *Accepted Manuscript* with the edited and formatted *Advance Article* as soon as it is available.

You can find more information about *Accepted Manuscripts* in the Information for Authors.

Please note that technical editing may introduce minor changes to the text and/or graphics, which may alter content. The journal's standard Terms & Conditions and the Ethical guidelines still apply. In no event shall the Royal Society of Chemistry be held responsible for any errors or omissions in this *Accepted Manuscript* or any consequences arising from the use of any information it contains.

ROYAL SOCIETY OF CHEMISTRY

www.rsc.org/pccp

Graphic abstract

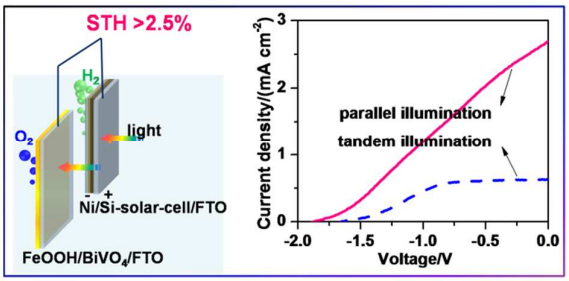

Overall water splitting with STH efficiency exceeding 2.5% using an all earth-abundant dual-photoelectrode device under parallel illumination without bias

Cite this: DOI: 10.1039/c0xx00000x

www.rsc.org/xxxxxx

PAPET

Solar-to-hydrogen Efficiency Exceeding 2.5% Achieved for Overall Water Splitting with All Earth-abundant Dual-photoelectrode

Chunmei Ding, Wei Qin, Nan Wang, Guiji Liu, Zhiliang Wang, Pengli Yan, Jingying Shi*, Can Li*

Received (in XXX, XXX) Xth XXXXXXXXX 20XX, Accepted Xth XXXXXXXXX 20XX
DOI: 10.1039/b000000x

The solar-to-hydrogen (STH) efficiency of a traditional mono-photoelectrode photoelectrochemical water splitting system has long been limited as large external bias is required. Herein, overall water splitting with STH efficiency exceeding 2.5% was achieved using a self-biased photoelectrochemical-photovoltaic coupled system consisting of all earth-abundant photoanode and Si-solar-cell-based photocathode connected in series under parallel illumination. We found that parallel irradiation mode shows higher efficiency than tandem illumination especially for photoanodes with wide light absorption range, probably as the driving force for water splitting reaction is larger and the photovoltage loss is smaller in the former. This work essentially takes advantage of tandem solar cell which can enhance the solar-to-electricity efficiency from another point of view.

Introduction

Photoelectrochemical (PEC) water splitting is one of the most promising strategies for solar fuel production.[1-5] Many materials with wide light absorption range such as $BiVO_4$[6-11], Fe_2O_3[12-14], Cu_2O[15-16], Ta_3N_5[17-21], $LaTiO_2N$[22-23] and Si[24-25] have been investigated as photoelectrodes in traditional mono-photoelectrode vs. Pt counter electrode systems. Despite of great efforts such as loading cocatalysts, doping with other elements, controlling morphologies, combining with other semiconductors and employing new fabrication methods to enhance the PEC performance of the photoelectrode, the solar-to-hydrogen (STH) efficiency for an individual photoelectrode is yet less than 1.8%, because large external bias is required for overall water splitting.[7-11, 14-21, 26-31] Therefore, it is highly desired to develop novel approaches for efficient PEC water splitting without external bias.

Constructing dual-photoelectrode system to use the Fermi level difference (ΔE_f) between them is a feasible solution. But it's not easy to fabricate two photoelectrodes well-matched in the same electrolyte, and the STH efficiency reported so far is quite low (< 0.1%)[11, 32-35], because the photovoltage is usually too small to overcome the overpotential of the reaction at the electrode. Photovoltaic-electrolysis (PV-EL) technology is more efficient but usually requires complicated setups and solar cells with rather high open-circuit voltage (V_{oc}) of at least 2.0 V[36-42]. Moreover, the water splitting ability of the system is mainly determined by the V_{oc} of the PV cell in a PV-EL system. However, if the PV cell is coupled with a semiconductor photoanode to construct a photovoltaic-PEC (PV-PEC) device, water oxidation reaction will take place on the photoanode surface, and thus the oxidant is the photogenerated hole whose energy can be very positive as it is determined by the valence band edge of the photoanode assisted by the PV cell. The most efficient PV-PEC system for water splitting reported so far consists of a p-$GaInP_2$ photocathode in contact with a GaAs solar cell connected with a Pt counter electrode.[43] While, these materials are high cost, toxic and unstable. In other reports, a solar cell was simply connected in the outer circuit of a PEC cell[44-47], directly deposited with water splitting photocatalyst[48-50] or combined with photocatalysts in tandem[9, 51-52]. The efficiency of such a tandem or monolithic configuration is limited because it is difficult to optimize performances of solar cell and photocatalyst layers with complementary light absorption.[51-53] Although a high efficiency was achieved recently[9], their device still has flaws: Firstly, the efficiency should be quiet low if other materials with a narrower band gap were used using their configuration; Secondly, the fabrication method of the semiconductor layer is limited as Si-cell cannot tolerate high temperature or any other harsh conditions; Lastly, the counter electrode they used is novel metal Pt which is unfavourable considering the cost.

Herein, we focus on the PV-PEC strategy which combines advantages of PEC and PV-EL systems. Overall water splitting with STH efficiency exceeding 2.5%, much higher than that of traditional mono-photoelectrode PEC and photocatalytic water splitting systems reported to date, was achieved with a self-biased dual-photoelectrode device. Coupling with semiconductor photoanode like $BiVO_4$, a Si solar cell (triple or double junction Si cell) was employed as photocathode. The decoupling of the PV cell and the PEC part in a PV-PEC system using a dual-photoelectrode configuration is convenient for the fabrication and optimization of them. And noble metal Pt electrode is avoided and all materials are earth-abundant and environmentally benign. Besides, illumination mode was found to be important for enhancing the efficiency of the system.

Results and discussion

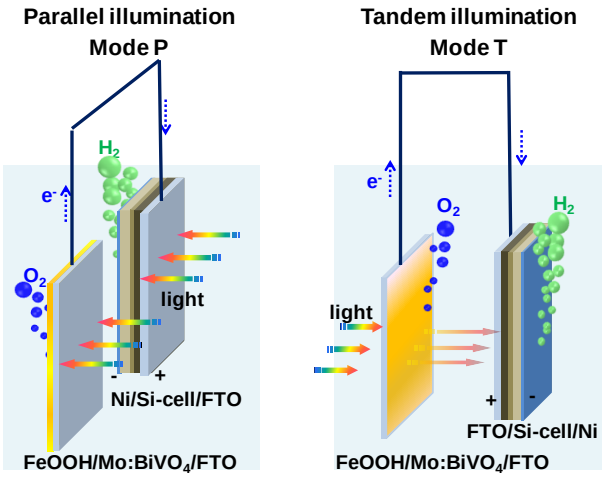

Fig. 1 A schematic description of the dual-photoelectrode device photoanode vs. Si-solar-cell-based photocathode for direct PEC water splitting under parallel (Mode P) and tandem (Mode T) illumination.

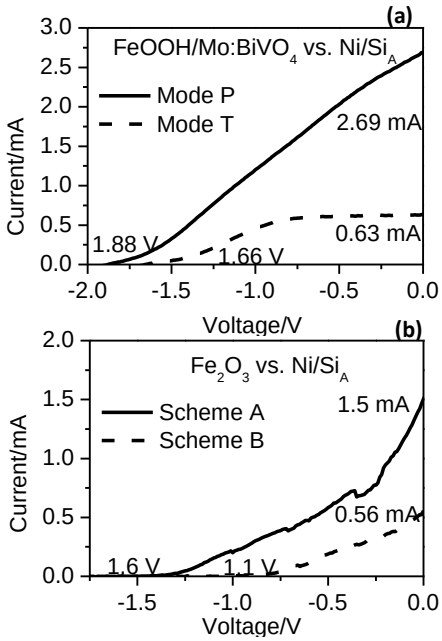

Fig. 2 I-V curves of $FeOOH/Mo:BiVO_4$, Fe_2O_3 photoanodes vs. Ni/Si_A in Modes P and T. Light source: AM 1.5G sunlight simulator (100 mW cm^{-2}); Scanning rate: 10 mV s^{-1}; Electrolyte: 0.5 M sodium phosphate (pH 7); Electrode areas: $FeOOH/Mo:BiVO_4$ or Fe_2O_3 1 cm^2 and Ni/Si_A 0.5 cm^2.

Fig. 1 schematically shows that a Si solar cell was applied as photocathode coupled with a photoanode in two illumination modes, one is parallel illumination (denoted as Mode P) with two beams of light and the other is tandem illumination (Mode T) with one beam of light incident from the photoanode side. Two Si solar cells (denoted as Si_A and Si_B, Fig. S1) with different V_{oc} and comparable short-circuit currents J_{sc} were used for comparison, and Ni cocatalyst was deposited on the surface of the Si cell to protect it from corrosion in the electrolyte and reduce the proton reduction potential. Fig. 2 (a) shows that the J_{sc} are 2.69 mA and 0.63 mA, respectively, when coupling Si_A with $FeOOH/Mo:BiVO_4$ photoanode in Modes P and T. The STH efficiency of Mode P calculated from J_{sc} is 2.21%, which is about 3 times of that of Mode T (0.77%). Similar results were obtained when changing the area of Si_A (Fig. S2). The V_{oc} of the coupled system in Mode P is 1.88 V which greater than that of Mode T, leading to the higher efficiency of Mode P. Fe_2O_3 photoanode was also coupled with Si_A likewise in two modes. Fig. 2 (b) shows that the J_{sc} of the system in Modes P and T are 1.5 mA and 0.56 mA, respectively. The corresponding STH efficiency of Mode P is 1.8 times of that of Mode T. The V_{oc} difference between Modes P and T is 0.5 V which brings about the big difference in STH efficiency. The comparison of the photocurrent under continuous irradiation between Modes P and T shows the same trend (Fig. S3).

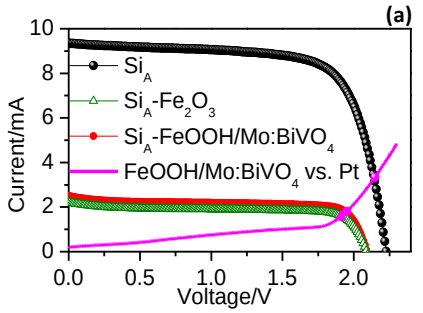

	V_{oc}/V	J_{sc}/mA
Si_A	2.23	9.4
Si_A-$FeOOH/Mo:BiVO_4$	2.09	2.5
Si_A-Fe_2O_3	2.09	2.2

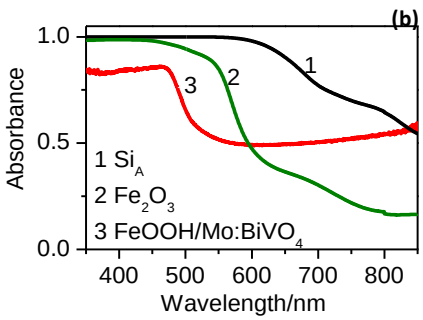

Fig. 3 (a) I-V curves, V_{oc} and J_{sc} of Si_A under full spectrum illumination and illuminated behind $FeOOH/Mo:BiVO_4$, Fe_2O_3 electrodes, and the average I-V curve of $FeOOH/Mo:BiVO_4$ (1 cm^2) vs. Pt two-electrode system, and (b) UV-visible absorption spectra of Si_A cell, Fe_2O_3, $FeOOH/Mo:BiVO_4$ photoanode. Electrolyte: 0.5 M sodium phosphate (pH 7); Light source: AM 1.5G sunlight simulator (100 mW cm^{-2}), Electrode area: Si_A 1 cm^2.

Results in Fig. 3 can partly explain the efficiency difference between Modes P and T. As shown in Fig. 3 (a), the efficiency of Si_A is dramatically reduced if the incident light is firstly absorbed by a photoanode. The J_{sc} of Si_A drops from 9.4 mA to only 2.5 mA and 2.2 mA for $FeOOH/Mo:BiVO_4$ and Fe_2O_3, respectively. And the V_{oc} is reduced by 0.14 V. The solid line is the average I-V curve of $FeOOH/Mo:BiVO_4$ electrode vs. Pt counter electrode in a two-electrode system. Its intersections with the I-V curves of Si_A are approximately the working points of the coupled system. The working photocurrent is obviously reduced when the light is incident through a photoelectrode. Fig. 3 (b) shows that the light absorption band edge of $FeOOH/Mo:BiVO_4$ and Fe_2O_3 are about

540 nm and 620 nm, respectively, and Si_A shows light absorption until 850 nm. Thus, after absorption and scattering by the photoanode, only a small portion of long wavelength photons are left for Si_A, resulting in a great decrease of the efficiency of Si_A. This suggests that the match of the light absorption of the photoanode and the solar cell is very important for achieving high efficiency of a PV-PEC device. In other words, illumination mode is important to optimize the efficiency. For photoanodes with wide light absorption range, dual-photoelectrode system under parallel illumination is demonstrated to be superior to those under tandem illumination and may be more efficient than the previous reported monolithic forms[9, 48-52]. Essentially, this is not contradictory to that tandem solar cell can enhance the solar-to-electricity efficiency but takes advantage of tandem solar cell technology from another point view.

Table 1 Results of the analysis of the photovoltage loss of the coupled system Si_A vs. FeOOH/Mo:$BiVO_4$ and Fe_2O_3 photoanodes in Modes P and T. V_{oc} is the open voltage of the coupled system, $V_{oc\text{-}Si}$ is the open voltage of Si_A itself, and V_{loss} is the photovoltage loss of the coupled system ($V_{loss} = V_{oc\text{-}Si} - V_{oc}$).

	Mode P			Mode T		
	$V_{oc\text{-}P}$ /V	$V_{oc\text{-}Si\text{-}P}$ /V	$V_{loss\text{-}P}$ /V	$V_{oc\text{-}T}$ /V	$V_{oc\text{-}Si\text{-}T}$ /V	$V_{loss\text{-}T}$ /V
Si_A vs. FeOOH/Mo:$BiVO_4$	1.88	2.23	0.35	1.66	2.09	0.43
Si_A vs. Fe_2O_3	1.6	2.23	0.63	1.1	2.09	0.99

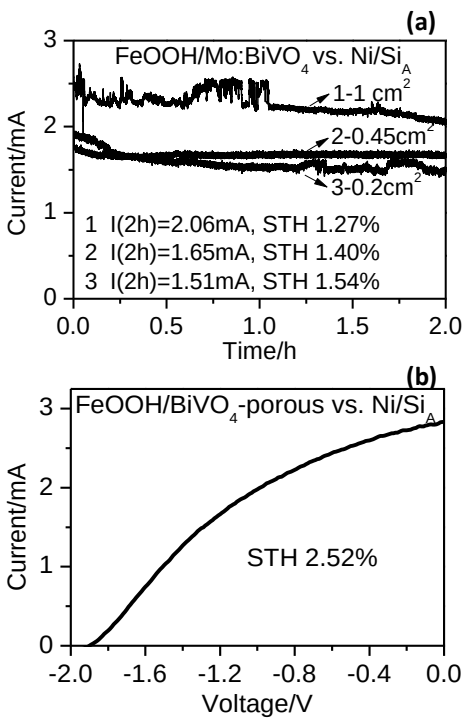

Fig. 4 (a) Short-circuit I-t curves of FeOOH/Mo:$BiVO_4$ photoanode (1 cm^2) vs. Ni/Si_A photocathode with different areas(1, 1 cm^2; 2, 0.45 cm^2; 3, 0.2 cm^2) in Mode P, and (b) the I-V curve of the FeOOH/$BiVO_4$-porous photoanode (0.98 cm^2) vs. Ni/Si_A (0.4 cm^2) in Mode P. Light source: AM 1.5G sunlight simulator (100 mW cm^{-2}); Scanning rate: 10 mV s^{-1}; Electrolyte: 0.5 M sodium phosphate (pH 7).

Table 1 shows the analysis of the photovoltage loss (V_{loss}) of Si_A vs. FeOOH/Mo:$BiVO_4$ and Fe_2O_3 photoanodes in Modes P and T. For FeOOH/Mo:$BiVO_4$, the measured V_{oc} of the device in Mode P ($V_{oc\text{-}P}$) is 1.88 V and the V_{oc} of Si_A itself ($V_{oc\text{-}Si}$) is 2.23 V, thus the V_{loss} of the device in Mode P ($V_{loss\text{-}P}$) is 0.35 V. V_{loss} is composed of two parts: one is the bias required to overcome the overpotential and compensate for the energy deficiency of the photoanode for overall water splitting, the other is the voltage loss due to the resistances of the photoanode, the Si-cell, the electrolyte as well as photoelectrode-cocatalyst and electrode-electrolyte interfaces. We previously found that the minimum bias required for cocatalyst/$BiVO_4$ photoanode to realize overall water splitting is about 0.3 V.[9] Namely, the voltage loss due to the coupling between FeOOH/Mo:$BiVO_4$ and Si_A is negligible, only 0.05 V, indicating the successful coupling between the photoanode and Si_A in Mode P. In contrast, the V_{loss} in Mode T ($V_{loss\text{-}T}$) is 0.43 V, larger than $V_{loss\text{-}P}$ by 80 mV. Similarly, $V_{loss\text{-}T}$ is larger than $V_{loss\text{-}P}$ by 360 mV in the case of Fe_2O_3. And similar results were also obtained for WO_3 photoanode (Table S1). Thus, it is inferred that more charge carriers are generated and survived after recombination in Mode P, which leads to a higher efficiency. This may be ascribed to the larger driving force V_{oc} and the better match of carrier flux between the photoanode and the photocathode in Mode P.

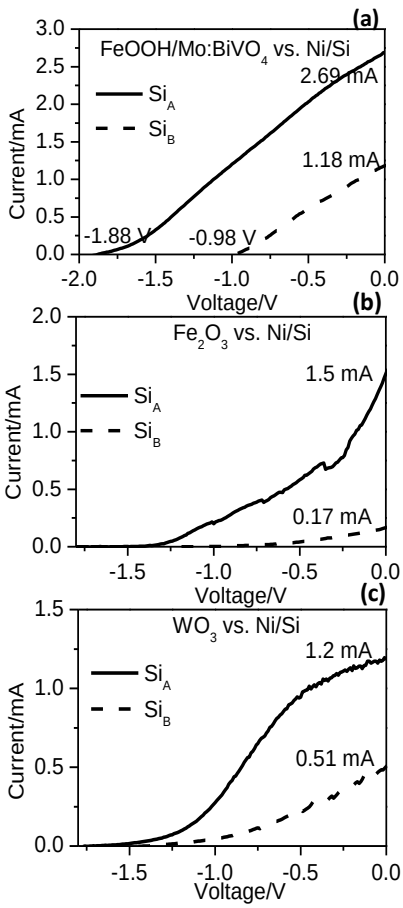

Fig. 5 I-V curves of Ni/Si_A or Ni/Si_B vs. (a) FeOOH/Mo:$BiVO_4$ (b) Fe_2O_3 and (c) WO_3 photoanodes in Mode P. Light source: AM 1.5G sunlight simulator (100 mW cm^{-2}); Scanning rate: 10 mV s^{-1}; Electrolyte: 0.5 M sodium phosphate (pH 7); Electrode areas: FeOOH/Mo:$BiVO_4$, Fe_2O_3 and WO_3 1 cm^2 and Ni/Si 0.5 cm^2.

Fig. 3 also indicates that the photocurrent of Si_A photocathode

is much higher than that of the photoanode, which means the hole flux from Si_A is largely excessive to the electron flux from the photoanode. In order to optimize the efficiency of the system, the charge flux of two photoelectrodes should be matched via changing the ratio of electrode areas or thickness of the photoanode. Fig. 4 (a) shows that the STH efficiency (calculated from the average current in 2 h) increases from 1.27% to 1.51% when the area of Si_A is decreased from 1 cm^2 to 0.2 cm^2. On the premise of providing enough hole flux, smaller Si_A means less light energy consumption and higher efficiency of the whole device. The efficiency of the system can also be improved if the photocurrent of the photoanode is increased. Fig. 4 (b) shows that the STH efficiency of the device $FeOOH/BiVO_4$-porous vs. Ni/Si_A reaches 2.52% via using a more efficient $FeOOH/BiVO_4$-porous photoanode (Fig. S4) prepared as recently reported[8]. Undoubtedly, the efficiency is expected to be higher if the PEC performance of the photoanode is further enhanced.

Since E_{CB} of $BiVO_4$ is only slightly lower than the proton reduction potential,[54] another Si solar cell (Si_B) with a smaller V_{oc} (1.22 V, Fig. S1) was coupled with $FeOOH/Mo:BiVO_4$ photoanode for comparison. Fig. 5 (a) shows that the obtained photocurrent of the system with Ni/Si_B is much lower than that with Ni/Si_A. Fe_2O_3 and WO_3 photoanodes with more positive E_{CB} than $BiVO_4$ were also coupled with Ni/Si_A and Ni/Si_B, respectively. As shown in Fig. 5 (b, c), the J_{sc} of Fe_2O_3 vs. Ni/Si_A is nearly 9 times of that of using Ni/Si_B. That is because Fe_2O_3 has a large overpotential for water oxidation and a large external bias is required.[13, 55] For WO_3, the J_{sc} of the system with Ni/Si_A is also higher than that of using Ni/Si_B. In brief, efficient overall water splitting can also be achieved using a Si cell with V_{oc} below 1.23 V, which is impossible in PV-EL system. While Si_B with smaller V_{oc} will result a low efficiency if the E_{CB} of the photoanode is too positive or the water oxidation overpotential is too large. In this case, loading efficient cocatalysts on the photoelectrode will be necessary to enhance the photocurrent and reduce the overpotential for higher efficiency.

Gas evolutions from the $FeOOH/Mo:BiVO_4$ vs. Ni/Si-cell system were determined. Fig. 6 (a, b) shows that H_2 and O_2 can be produced efficiently from the system in stoichiometric ratio without external bias. To evaluate the contribution of the photoanode in the PV-PEC system, we replaced it with a CoPi electrode which has been developed as one of the most efficient water oxidation electrocatalysts in neutral phosphate electrolyte.[56] Fig. 6 (c, d) shows that the activity of the resulting PV-EL system CoPi vs. Si-cell is much lower than that of $FeOOH/Mo:BiVO_4$ vs. Ni/Si-cell. The STH efficiency of $FeOOH/Mo:BiVO_4$ vs. Ni/Si-cell photoanode is about 3 (for Ni/Si_A) and 8 (for Ni/Si_B) times of that of using CoPi, indicating the potential advantage of PV-PEC systems over PV-EL systems. To reveal the role of the Si-cell in the coupled system, we replaced the Si-cell with a Pt modified p-Si photocathode (Pt/p-Si NW) fabricated from a Si single crystal wafer as schematically shown in Fig. 7 (a). The V_{oc} of the dual-photoelectrode system is 0.31 V and the J_{sc} is 20 μA (Fig. 7(b)), indicating that photoelectrons can transfer from the photoanode to the photocathode without external bias but the STH efficiency is only about 0.01%, much lower than that of using Si-cell photocathode. Fig. 7 (c, d) shows that O_2 and H_2 can be produced from the $FeOOH/Mo:BiVO_4$ vs. Pt/p-Si NW system under a bias of 0 V or 0.2 V, but the activities are quite low. And the H_2/O_2 ratio deviates from stoichiometric value due to the corrosion of p-Si and the H_2 evolution even exceeds the amount of e/2 probably because of the reaction of Si with H_2O and reverse reactions. When using the $Pt/TiO_2/Ti/p$-Si electrode which is more active and corrosion resistant[57], the activity is still low despite a slight increase (Fig. S5). The reason may be that the driving force ΔE_f between two photoelectrodes is too small and limits the efficiency of the whole system. In contrast, in the PV-PEC system, the photovoltage generated from the PEC and PV systems can easily meet the requirement for overall water splitting reaction.

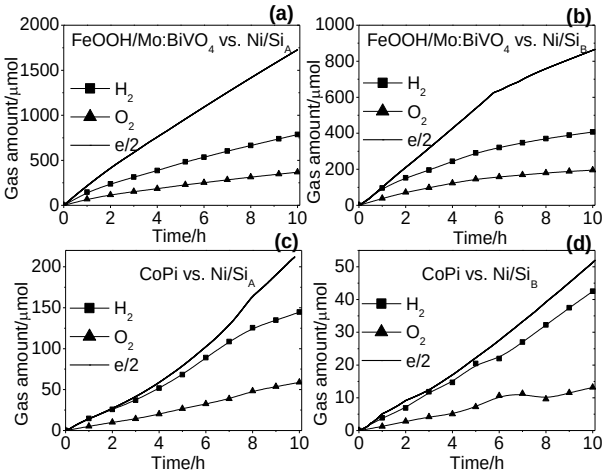

Fig. 6 Time courses of gas evolutions and corresponding e/2 amounts of $FeOOH/Mo:BiVO_4$ photoanode vs. Si_A (a) and Si_B (b) coupled systems in Mode P, and those of CoPi electrode vs. Si_A (c) and Si_B (d). Light source: 300 W Xe lamp; Scanning rate: 20 mV s^{-1}; Electrolyte: 0.5 M sodium phosphate (pH 7); Electrode areas: CoPi and $FeOOH/Mo:BiVO_4$ 1 cm^2 and Ni/Si 0.5 cm^2.

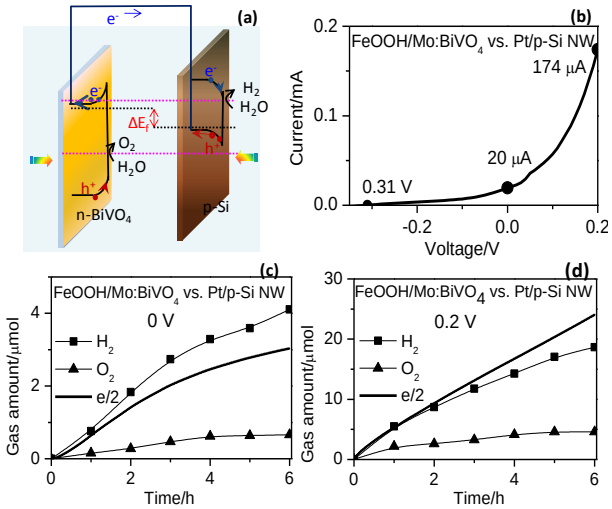

Fig. 7 (a) A schematic description of the dual-electrode system with $BiVO_4$ photoanode vs. p-Si photocathode for direct PEC water splitting, (b) I-V curve of the two-electrode system $FeOOH/Mo:BiVO_4$ vs. Pt/p-Si NW photocathode under AM 1.5G sunlight illumination (100 mW cm^{-2}), and (c, d) time courses of gas evolution and corresponding e/2 amounts of $FeOOH/Mo:BiVO_4$ photoanode vs. Pt/p-Si NW under 300 W Xe lamp irradiation with a bias of 0 V and 0.2 V. Electrolyte: 0.5 M sodium

phosphate (pH 7); Electrode areas: FeOOH/Mo:$BiVO_4$ 1 cm^2 and Pt/p-Si photocathode 1 cm^2; Scanning rate: 10 mV s^{-1}.

Conclusions

A self-biased dual-illumination PEC device consisting of a semiconductor photoanode and a Si-solar-cell based photocathode connected in series was constructed for overall water splitting. The STH efficiency of the FeOOH/$BiVO_4$ vs. Si-cell system can exceed 2.5%, much higher than that of traditional mono-photoelectrode PEC and photocatalytic water splitting systems to date. In this configuration, noble metal electrode is avoided and all materials are earth-abundant and environmentally benign. And the decoupling of the PV cell and the PEC part using a dual-photoelectrode configuration is convenient for the fabrication and optimization of them. It is found that parallel illumination mode shows higher efficiency than tandem irradiation for photoanodes with wide light absorption range, probably as the driving force for water splitting reaction is larger and the photovoltage loss is smaller in the former. This indicates that a dual-photoelectrode PV-PEC device under parallel illumination is superior to those in tandem or monolithic forms. From another point of view, this work essentially takes advantage of tandem solar cell technology which can enhance the solar-to-electricity efficiency. Besides, the efficiency is obviously decreased when the photoanode is replaced by a CoPi electrode or when Si-cell is substituted by a p-Si photocathode. This clarifies roles of the photoanode and the solar cell in the coupled system and demonstrates the potential advantage of PV-PEC systems over PV-EL systems.

Experimental Section

All chemicals were analytical grade and were used as purchased without further purification. Solutions were prepared using high purity water (resistivity > 18 MΩ·cm). The FTO (fluorine-doped tin oxide, < 14 Ω/square) conductive glass was purchased from Nippon Sheet Glass Company (Japan) and was ultrasonic cleaned with acetone, isopropanol, ethanol and deionized water for 20 min each prior to use.

Fabrication of Ni/Si-cell, FeOOH/Mo:$BiVO_4$, Fe_2O_3, WO_3, CoPi, and Pt/p-Si electrodes: Si solar cells used for photocathode fabrication are commercial Si solar cells (Hanergy Companay, China). Two types of Si-cell with different V_{oc} and J_{sc} (Fig. S1): one is triple-junction Si_A composed of one layer of amorphous Si and two layers of nanocrystal Si and the other is double-junction Si_B, were used. The anode side of the Si-cell was connected with the photoanode using Cu wire and Ag conductive adhesive. The cathode side is deposited with Ni cocatalyst (about 100 nm in thickness) by d.c. reactive magnetron sputtering. The Si-cell was illuminated from FTO side. Mo:$BiVO_4$ electrodes were prepared by a modified electrodeposition method.[10, 54] To stabilize and enhance the PEC performance, FeOOH cocatalyst was deposited on the surface of Mo:$BiVO_4$ photoelectrode via PEC oxidation of $FeCl_2 \cdot xH_2O$ (99%, Alfa Aesar)[10] (Fig. S4, Electronic Supplementary Information). The FeOOH/$BiVO_4$-pourous electrode was prepared as recently reported.[8] Fe_2O_3 electrodes were prepared by chemical bath deposition and annealing method, WO_3 electrodes were fabricated by d.c. reactive magnetron sputtering system, and CoPi electrodes were prepared by electrodeposition (Electronic Supplementary Information). Pt/p-Si NW and Pt/TiO_2/Ti/p-Si photocathodes were prepared from p-Si (100) wafers as reported[57-58], and both of them show high cathodic photocurrent (Fig. S5, S6).

PEC characterizations and measurements of gas evolutions: Photocurrent measurements were performed in a two-electrode cell with Pt (2 cm × 3 cm) or a three-electrode setup with SCE reference electrode (0.242 V vs. NHE). The electrolyte was purged with Ar for 30 min before PEC measurements and bubbled with Ar during the tests. The light source was an AM 1.5G sunlight simulator (100 mW cm^{-2}) unless otherwise stated. Measurements of gas evolutions were carried out in a two-electrode cell as reported before.[54] STH efficiencies were calculated according to equation (1)[1] supposing the Faradic efficiency (η_F) is 100%:

$$STH = \frac{\eta_F \times J_{sc}\,(mA) \times 1.23V}{100\,mW \cdot cm^{-2} \times (Area_{BiVO_4}(cm^2) + Area_{Si}(cm^2))} \times 100\% \quad (1)$$

Acknowledgements

This work was financially supported by the National Basic Research Program of the Ministry of Science and Technology, China (Grant 2014CB239400); National Natural Science Foundation of China (No. 21061140361, 21090340) and Solar Energy Action Plan of Chinese Academy of Sciences (No. KGCX2-YW-399+7-3).

Notes and references

** To whom correspondence should be addressed:*
Email: canli@dicp.ac.cn; jingyingshi@dicp.ac.cn;
Tel: 86-411-84379070; Fax: 86-411-84694447; Home page: http://www.canli.dicp.ac.cn

† Electronic Supplementary Information (ESI) available: [Experimental details and other supporting data]. See DOI: 10.1039/b000000x/

References:

[1] Z. B. Chen; T. F. Jaramillo; T. G. Deutsch; A. Kleiman-Shwarsctein; A. J. Forman; N. Gaillard; R. Garland; K. Takanabe; C. Heske; M. Sunkara; Others. Accelerating materials development for photoelectrochemical hydrogen production: Standards for methods, definitions, and reporting protocols, **J. Mater. Res.**, **2010**, 25(1), 3-16.

[2] M. G. Walter; E. L. Warren; J. R. McKone; S. W. Boettcher; Q. Mi; E. A. Santori; N. S. Lewis. Solar water splitting cells, **Chem. Rev.**, **2010**, 110(11), 6446-6473.

[3] B. A. Pinaud; J. D. Benck; L. C. Seitz; A. J. Forman; Z. B. Chen; T. G. Deutsch; B. D. James; K. N. Baum; G. N. Baum; S. Ardo; H. L. Wang; E. Miller; T. F. Jaramillo. Technical and economic feasibility of centralized facilities for solar hydrogen production via photocatalysis and photoelectrochemistry, **Energy Environ. Sci.**, **2013**, 6(7), 1983-2002.

[4] R. Abe. Recent progress on photocatalytic and photoelectrochemical water splitting under visible light irradiation, **J. Photochem. Photobiol., C: Photochemistry Reviews**, **2010**, 11(4), 179-209.

[5] K. S. Joya; Y. F. Joya; K. Ocakoglu; R. van de Krol. Water-Splitting Catalysis and Solar Fuel Devices: Artificial Leaves on the Move, **Angew. Chem. Int. Ed.**, **2013**, 52(40), 10426-10437.

[6] Yiseul Park; Kenneth J. McDonald; Kyoung-Shin Choi. Progress in bismuth vanadate photoanodes for use in solar water oxidation, **Chem. Soc. Rev**, **2013**, 42, 2321-2337.

[7] KPS Parmar; H. J. Kang; A. Bist; P. Dua; J. S. Jang; J. S. Lee. Photocatalytic and Photoelectrochemical Water Oxidation over

Metal-Doped Monoclinic BiVO4 Photoanodes, **ChemSusChem**, **2012**, 5(10), 1926-1934.

[8] Tae Woo Kim; Kyoung-Shin Choi. Nanoporous BiVO4 Photoanodes with Dual-Layer Oxygen Evolution Catalysts for Solar Water Splitting, **Science**, **2014**, 10.1126/science.1246913.

[9] Fatwa F. Abdi; Lihao Han; Arno H. M. Smets; Miro Zeman; Bernard Dam; Roel van de Krol. Efficient solar water splitting by enhanced charge separation in a bismuth vanadate-silicon tandem photoelectrode, **Nat. Commun.**, **2013**, 4(2195), 10-1038.

[10] Jason A. Seabold; Kyoung-Shin Choi. Efficient and Stable Photo-Oxidation of Water by a Bismuth Vanadate Photoanode Coupled with an Iron Oxyhydroxide Oxygen Evolution Catalyst, **J. Am. Chem. Soc.**, **2012**, 134(4), 2186-2192.

[11] Q. Jia; K. Iwashina; A. Kudo. Facile fabrication of an efficient BiVO4 thin film electrode for water splitting under visible light irradiation, **PNAS**, **2012**, 109(29), 11564-11569.

[12] C. Du; X. G. Yang; M. T. Mayer; H. Hoyt; J. Xie; G. McMahon; G. Bischoping; D. W. Wang. Hematite-Based Water Splitting with Low Turn-On Voltages, **Angew. Chem. Int. Ed.**, **2013**, 52(48), 12692-12695.

[13] Dapeng Cao; Wenjun Luo; Jianyong Feng; Xin Zhao; Zhaosheng Li; Zhigang Zou. Cathodic shift of onset potential for water oxidation on a Ti4+ doped Fe2O3 photoanode by suppressing back reaction, **Energy Environ. Sci.**, **2014**, 7, 752-759.

[14] Scott C. Warren; Kislon Voïtchovsky; Hen Dotan; Celine M. Leroy; Maurin Cornuz; Francesco Stellacci; Cécile Hébert; Avner Rothschild; Michael Grätzel. Identifying champion nanostructures for solar water-splitting, **Nature Materials**, **2013**, 12, 842-849.

[15] Adriana Paracchino; Vincent Laporte; Kevin Sivula; Michael Grätzel; Elijah Thimsen. Highly active oxide photocathode for photoelectrochemical water reduction, **Nature Materials**, **2011**, 10, 456-461.

[16] S. David Tilley; Marcel Schreier; João Azevedo; Morgan Stefi K; And Michael Graetzel. Ruthenium Oxide Hydrogen Evolution Catalysis on Composite Cuprous Oxide Water-Splitting Photocathodes, **Adv. Funct. Mater.**, **2013**, 24(3), 303-311.

[17] Mingxue Li; Wenjun Luo; Dapeng Cao; Xin Zhao; Zhaosheng Li; Tao Yu; Zhigang Zou. A Cocatalyst-Loaded Ta3N5 Photoanode with a High Solar Photocurrent for Water Splitting upon Facile Removal of the Surface Layer, **Angew. Chem. Int. Ed.**, **2013**, 52, 1-6.

[18] J. G. Hou; Z. Wang; C. Yang; H. J. Cheng; S. Q. Jiao; H. M. Zhu. Cobalt-bilayer catalyst decorated Ta3N5 nanorod arrays as integrated electrodes for photoelectrochemical water oxidation, **Energy Environ. Sci.**, **2013**, 6(11), 3322-3330.

[19] Y. B. Li; T. Takata; D. Cha; K. Takanabe; T. Minegishi; J. Kubota; K. Domen. Vertically Aligned Ta3N5 Nanorod Arrays for Solar-Driven Photoelectrochemical Water Splitting, **Adv. Mater.**, **2013**, 25(1), 125-131.

[20] M. J. Liao; J. Y. Feng; W. J. Luo; Z. Q. Wang; J. Y. Zhang; Z. S. Li; T. Yu; Z. G. Zou. Co3O4 Nanoparticles as Robust Water Oxidation Catalysts Towards Remarkably Enhanced Photostability of a Ta3N5 Photoanode, **Adv. Funct. Mater.**, **2012**, 22(14), 3066-3074.

[21] Y. B. Li; L. Zhang; A. Torres-Pardo; J. M. Gonzalez-Calbet; Y. H. Ma; P. Oleynikov; O. Terasaki; S. Asahina; M. Shima; D. Cha; L. Zhao; K. Takanabe; J. Kubota; K. Domen. Cobalt phosphate-modified barium-doped tantalum nitride nanorod photoanode with 1.5% solar energy conversion efficiency, **Nat. Commun.**, **2013**, 4(2566), 10-1038.

[22] T. Minegishi; N. Nishimura; J. Kubota; K. Domen. Photoelectrochemical properties of LaTiO2N electrodes prepared by particle transfer for sunlight-driven water splitting, **Chem. Sci.**, **2013**, 4(3), 1120-1124.

[23] Jianyong Feng; Wenjun Luo; Tao Fang; Hao Lv; Zhiqiang Wang; Jian Gao; Wenming Liu; Tao Yu; Zhaosheng Li; Zhigang Zou. Highly Photo-Responsive LaTiO2N Photoanodes by Improvement of Charge Carrier Transport among Film Particles, **Adv. Funct. Mater.**, **2014**, DOI: 10.1002/adfm.201304046.

[24] Michael J. Kenney; Ming Gong; Yanguang Li; Justin Z. Wu; Ju Feng; Mario Lanza; Hongjie Dai. High-Performance Silicon Photoanodes Passivated with Ultrathin Nickel Films for Water Oxidation, **Science**, **2013**, 342(6160), 836-840.

[25] Jinhui Yang; Karl Walczak; Eitan Anzenberg; Francesca Maria Toma; Guangbi Yuan; Jeffrey Beeman; Adam; Schwartzberg; Yongjing Lin; Mark Hettick; Ali Javey; Joel W. Ager; Junko Yano; Heinz Frei; Ian D. Sharp. Efficient and Sustained Photoelectrochemical Water Oxidation by Cobalt Oxide/Silicon Photoanodes with Nanotextured Interfaces, **J. Am. Chem. Soc.**, **2014**, 136(17), 6191-6194.

[26] M. Higashi; K. Domen; R. Abe. Highly Stable Water Splitting on Oxynitride TaON Photoanode System under Visible Light Irradiation, **J. Am. Chem. Soc.**, **2012**, 134(16), 6968-6971.

[27] S. K. Pilli; T. G. Deutsch; T. E. Furtak; J. A. Turner; L. D. Brown; A. M. Herring. Light induced water oxidation on cobalt-phosphate (Co-Pi) catalyst modified semi-transparent, porous SiO2-BiVO4 electrodes, **Phys. Chem. Chem. Phys.**, **2012**, 14(19), 7032-7039.

[28] S. P. Berglund; A. J. E. Rettie; S. Hoang; C. B. Mullins. Incorporation of Mo and W into nanostructured BiVO4 films for efficient photoelectrochemical water oxidation, **Phys. Chem. Chem. Phys.**, **2012**, 14(19), 7065-7075.

[29] R. Saito; Y. Miseki; K. Sayama. Highly efficient photoelectrochemical water splitting using a thin film photoanode of BiVO4/SnO2/WO3 multi-composite in a carbonate electrolyte, **Chem. Commun.**, **2012**, 48(32), 3833-3835.

[30] M. Higashi; K. Domen; R. Abe. Fabrication of efficient TaON and Ta3N5 photoanodes for water splitting under visible light irradiation, **Energy Environ. Sci.**, **2011**, 4(10), 4138-4147.

[31] A. Kay; I. Cesar; M. Gratzel. New benchmark for water photooxidation by nanostructured alpha-Fe2O3 films, **J. Am. Chem. Soc.**, **2006**, 128(49), 15714-15721.

[32] Q. P. Chen; J. H. Li; X. J. Li; K. Huang; B. X. Zhou; W. F. Shangguan. Self-Biasing Photoelectrochemical Cell for Spontaneous Overall Water Splitting under Visible-Light Illumination, **ChemSusChem**, **2013**, 6(7), 1276-1281.

[33] S. Ida; K. Yamada; T. Matsunaga; H. Hagiwara; Y. Matsumoto; T. Ishihara. Preparation of p-Type CaFe2O4 Photocathodes for Producing Hydrogen from Water, **J. Am. Chem. Soc.**, **2010**, 132(49), 17343-17345.

[34] Heli Wang; Todd Deutsch; John A. Turner. Direct Water Splitting under Visible Light with Nanostructured Hematite and WO3 Photoanodes and a GaInP2 Photocathode, **J. Electrochem. Soc.**, **2008**.

[35] W. B. Ingler; S. U. M. Khan. A Self-Driven p/n-Fe2O3 Tandem Photoelectrochemical Cell for Water Splitting, **Electrochem. Solid-State Lett.**, **2006**, 9(4), G144-G146.

[36] JJH Pijpers; M. T. Winkler; Y. Surendranath; T. Buonassisi; D. G. Nocera. Light-induced water oxidation at silicon electrodes functionalized with a cobalt oxygen-evolving catalyst, **PNAS**, **2011**, 108(25), 10056-10061.

[37] S. Eker; F. Kargi. Hydrogen gas production from electrohydrolysis of industrial wastewater organics by using photovoltaic cells (PVC), **Int. J. Hydrogen Energy**, **2010**, 35(23SI), 12761-12766.

[38] T. L. Gibson; N. A. Kelly. Optimization of solar powered hydrogen production using photovoltaic electrolysis devices, **Int. J. Hydrogen Energy**, **2008**, 33(21), 5931-5940.

[39] O. Khaselev; A. Bansal; J. A. Turner. High-efficiency integrated multijunction photovoltaic/electrolysis systems for hydrogen production, **Int. J. Hydrogen Energy**, **2001**, 26(2), 127-132.

[40] A. Dukic; M. Firak. Hydrogen production using alkaline electrolyzer and photovoltaic (PV) module, **Int. J. Hydrogen Energy**, **2011**, 36(13), 7799-7806.

[41] S. Y. Reece; J. A. Hamel; K. Sung; T. D. Jarvi; A. J. Esswein; JJH Pijpers; D. G. Nocera. Wireless Solar Water Splitting Using Silicon-Based Semiconductors and Earth-Abundant Catalysts, **Science**, **2011**, 334(6056), 645-648.

[42] T. Jesper Jacobsson; Viktor Fj Allstr Om; Martin Sahlberg; Marika Edoff; Tomas Edvinsson. A monolithic device for solar water splitting based on series interconnected thin film absorbers reaching over 10% solar-to-hydrogen efficiency, **Energy Environ. Sci.**, **2013**, 6, 3676-3683.

[43] O. Khaselev; J. A. Turner. A monolithic photovoltaic-photoelectrochemical device for hydrogen production via water splitting, **Science**, **1998**, 280(5362), 425-427.

[44] P. K. Shukla; R. K. Karn; A. K. Singh; O. N. Srivastava. Studies on PV assisted PEC solar cells for hydrogen production through photoelectrolysis of water, **Int. J. Hydrogen Energy**, **2002**, 27(2), 135-141.
[45] L. Andrade; R. Cruz; H. A. Ribeiro; A. Mendes. Impedance characterization of dye-sensitized solar cells in a tandem arrangement for hydrogen production by water splitting, **Int. J. Hydrogen Energy**, **2010**, 35(17SI), 8876-8883.
[46] A. Currao; V. R. Reddy; M. K. van Veen; R. E. I. Schropp; G. Calzaferri. Water splitting with silver chloride photoanodes and amorphous silicon solar cells, **Photochem. Photobiol. Sci.**, **2004**, 3(11-12), 1017-1025.
[47] J. Brillet; M. Cornuz; F. Le Formal; J. H. Yum; M. Gratzel; K. Sivula. Examining architectures of photoanode-photovoltaic tandem cells for solar water splitting, **J. Mater. Res.**, **2010**, 25(1), 17-24.
[48] E. L. Miller; R. E. Rocheleau; X. M. Deng. Design considerations for a hybrid amorphous silicon/photoelectrochemical multijunction cell for hydrogen production, **Int. J. Hydrogen Energy**, **2003**, 28(6), 615-623.
[49] A. Stavrides; A. Kunrath; J. Hu; R. Treglio; A. Feldman; B. Marsen; B. Cole; E. Miller; A. Madan. Use of amorphous silicon tandem junction solar cells for hydrogen production in a photoelectrochemical cell, **Proc. of SPIE**, **2006**, 6340(63400K), 1-8.
[50] F. Zhu; J. Hu; A. Kunrath; I. Matulionis; B. Marsen; B. Cole; E. Miller; A. Madan. a-SiC : H films used as photoelectrodes in a hybrid, thin-film silicon photoelectrochemical (PEC) cell for progress toward 10% solar-to hydrogen efficiency, **Proc. of SPIE**, **2007**, 6650(66500S), 1-9.
[51] J. Brillet; J. H. Yum; M. Cornuz; T. Hisatomi; R. Solarska; J. Augustynski; M. Graetzel; K. Sivula. Highly efficient water splitting by a dual-absorber tandem cell, **Nature Photonics**, **2012**, 6(12), 823-827.
[52] Lihao Han; Fatwa F. Abdi; Paula Perez Rodriguez; Bernard Dam; Roel Van; de Krol; Miro Zemana; Arno H. M. Smets. Optimization of Amorphous Silicon Double Junction Solar Cells for an Efficient Photoelectrochemical Water Splitting Device Based on Bismuth Vanadate Photoanode, **Phys. Chem. Chem. Phys.**, **2013**, 00, 1-3.
[53] Eric L. Miller; Bjorn Marsen Z; Daniela Paluselli; Richard Rocheleau. Optimization of Hybrid Photoelectrodes for Solar Water-Splitting, **Electrochem. Solid-State Lett.**, **2005**, 8(5), A247-A249.
[54] Chunmei Ding; Jingying Shi; Donge Wang; Guiji Liu; Fengqiang Xiong; Can Li. Visible light driven overall water splitting using cocatalyst/BiVO4 photoanode with minimized bias, **Phys. Chem. Chem. Phys.**, **2013**, 15, 4589-4595.
[55] S. C. Riha; B. M. Klahr; E. C. Tyo; S. Seifert; S. Vajda; M. J. Pellin; T. W. Hamann; ABF Martinson. Atomic Layer Deposition of a Submonolayer Catalyst for the Enhanced Photoelectrochemical Performance of Water Oxidation with Hematite, **ACS NANO**, **2013**, 7(3), 2396-2405.
[56] M. W. Kanan; D. G. Nocera. In situ formation of an oxygen-evolving catalyst in neutral water containing phosphate and Co2+, **Science**, **2008**, 321(5892), 1072-1075.
[57] Brian Seger; Thomas Pedersen; Anders B. Laursen; Peter C. K. Vesborg; Ole Hansen; Ib Chorkendorff. Using TiO2 as a Conductive Protective Layer for Photocathodic H2 Evolution, **J. Am. Chem. Soc**, **2013**, 135, 1057-1064.
[58] I. Oh; J. Kye; S. Hwang. Enhanced Photoelectrochemical Hydrogen Production from Silicon Nanowire Array Photocathode, **Nano Lett.**, **2012**, 12(1), 298-302.